ZnO hollow spheres arrayed molecularly-printed-polymer based selective electrochemical sensor for methyl-parathion pesticide detection

M. Daizy [a,b], M.R. Ali [a,b], M.S. Bacchu [a,b], M. Aly Saad Aly [c], M.Z.H. Khan [a,b,*]

[a] Department of Chemical Engineering, Jashore University of Science and Technology, Jashore 7408, Bangladesh
[b] Laboratory of Nano-bio and Advanced Materials Engineering (NAME), Jashore University of Science and Technology, Jashore 7408, Bangladesh
[c] Department of New Biology, Daegu Gyeongbuk Institute of Science and Technology (DGIST), 333 Techno jungang-daero, Daegu 42988, Republic of Korea

ARTICLE INFO

ABSTRACT

A highly sensitive electrochemical-based detector was fabricated to selectively sense methyl-parathion (MP). A Glassy carbon electrode (GCE) was functionalized with zinc oxide (ZnO) hollow spheres (ZnOHS) and a molecularly imprinted polymer (MIP) to form the developed sensor. Cyclic voltammetry (CV) was performed to synthesize a molecularly imprinted polymeric film on the ZnOHS modified GCE (GCE/ZnOHS) by electropolymerization of functional monomer, l-arginine (L-Arg), and template molecule, MP. The differential pulse voltammetry (DPV) was utilized to evaluate the efficiency of the electrochemical detection of MP under optimal conditions by the proposed sensor. The developed sensor recorded a good performance for detecting MP in the linear range of 5×10^{-9} to 0.1×10^{-4} mol L^{-1} ($R^2 = 0.985$) with a detection limit (S/N = 3) of 0.5×10^{-9} mol L^{-1} and sensitivity of 571 nA/μmolL^{-1} cm^{-2}. This electrochemical sensing system effectively detects MP in real samples with satisfactory recoveries of 90.4%, 91.9%, 118%, and 96.3% for fresh green beans, strawberry, tomato, and cabbage, respectively.

© 2021 Elsevier B.V. All rights reserved.

1. Introduction

In agriculture, more than half of crops are destroyed by pests at different stages of crop growth and harvesting which makes it very important to use pesticides to solve this problem (Mesterházy et al., 2020). Organophosphorus (OP) based pesticides are extensively used in agriculture and are playing an important role in increasing food production by protecting crops from harmful pests (Sakata, 2005; Yang et al., 2008). The toxic derivatives of OP-based pesticides include methyl-parathion (MP), parathion, paraoxon, malathion, fenitrothion, dichlorvos, and chlorpyrifos. MP is a highly toxic OP compound that is used as pesticide for several crops such as potatoes, cabbage, cereals, green beans, fruits, and sugarcane to enhance food production and pest control (De Souza and Machado, 2006; Silva et al., 2004; Xue et al., 2004). However, long-term use of MP in the treatment of crop disease led to the presence of its residues in nourishments. The presence of such deadly residues in nourishments is a major threat to human health (Huang et al., 2015; Mulchandani et al., 2001). MP also can act as irreversible acetylcholinesterase (AChE) inhibitor that prevents AChE from breaking down into choline and acetate. Thus, it accumulates in the human central nervous system as an intact state that leads to various diseases

such as headaches, hypotension, vomiting and can also lead to death (EPA, 2000; Liu and Lin, 2005). Thus, developing sensitive and sensitive methods for detecting MP in nourishments is necessary for human health and safety.

Several analytical techniques like high-performance liquid chromatography, mass spectrometry, gas chromatography assisted with mass-spectroscopy, immunoassay, and capillary electrophoresis were reported for the determination of MP (Anh et al., 2011; Barr et al., 2002; Shanker et al., 2001; Tomkins and Ilgner, 2002; Wang et al., 2001). Although these methods are highly effective in detecting MP, they are slow, expensive, not suitable for real-time detection, and further, require sample pretreatment. Alternatively, electrochemical techniques offer rapid, relatively low cost, highly sensitive, and selective detection capabilities (Sadik et al., 2003). Recently, substantial advancements in the molecular-imprinting process were observed for the electrochemical determination of various analytes owing to their strong attraction to template molecules (Kartal et al., 2019; Wang et al., 2019). The molecularly imprinted polymers (MIP) based sensors are formed by electro-polymerization of a functional monomer along with targeted template molecules to form monomer-template complexes. Once the template molecules are extracted, recognition cavities are formed on the sensor. The target template molecules are detected by MIP when they match the specific cavities (Uzun and Turner, 2016; Wang and Cao, 2015). MIP-based electrochemical detection systems offer the benefits of both electrochemical and MIP approaches (Gui et al., 2018). However, MIP sensors have some drawbacks such as low conductivity and low sensitivity that should be overcome (Tan et al., 2015). Various metal and metal oxides nanoparticles (Beluomini et al., 2017), nanotubes (Zhang et al., 2015a), and nanocomposites (Wang et al., 2019) were used to enlarge the surface area and conductivity of electrochemical sensors. Among the different types of metal oxide competitors, zinc oxide nanoparticles draw great attention in many current fields owing to their exceptional optical, surface, and electrical properties (Alenezi et al., 2014; Giahi et al., 2013). The different structural morphologies of ZnO nanostructures such as flowers, rods, wires, helices, hollow spheres may significantly influence the electrochemical behavior of the developed sensor (Wang et al., 2013; Zhang et al., 2015b). In addition, these diverse ranges of morphologies have a direct effect on the electrochemical response of sensors to detect chemical analytes (Hieu et al., 2016). Among them, ZnO hollow nanostructure morphology acquired considerable interest in electrochemical sensing applications because it provides large surface-area, chemical stability, superior electrical conductivity, and surface functionality (Alexander et al., 2019; Ameen et al., 2015). The high electrical conductivity of electrochemical sensors improves the sensor sensitivity and further provides a low detection-limit. Wang et al., 2020 prepared an electrochemical sensor based on MOF-derived NiO@ZnO hollow microspheres which presented a good electrochemical response for isoniazid detection (Wang et al., 2020). These work reports highlight the effect of ZnOHS on increasing the sensitivity of electrochemical sensors.

Here, we constructed a novel MIP-based electrochemical sensing mechanism to detect MP with high selectivity and sensitivity. ZnOHS were drop-casted on GCE to effectively increase the sensitivity of the sensor. A MIP film was formed onto the GCE/ZnOHS for the selective detection of the target analyte. Moreover, the prepared GCE/ZnOHS/MIP sensor effectively detects MP in real samples.

2. Experimental procedure

2.1. Chemicals and reagents

All purchased agents were at high purity, therefore no further purifying was required. MP (PESTANAL® analytical grade) was bought from Sigma Aldrich, (Germany). A solution of MP (0.5×10^{-3} mol/L) was obtained in ethanol. L-arginine (L-Arg), and phosphate buffer saline (PBS) of 1×10^{-2} mol/L (pH level of 7.4) were bought from Sigma Aldrich (China). Zinc nitrate hexahydrate ($Zn(NO_3)_2 \cdot 6H_2O$) and tri-sodium citrate dehydrate ($C_6H_5Na_3O_7 \cdot 2H_2O$) were bought from Merck (Germany). Hexamine ($C_6H_{12}N_4$) was purchased from PT.SMART LAB (Indonesia). A supporting electrolyte solution that contains 5 mM of potassium-ferricyanide and potassium-ferrocyanide (1:1) along with 0.1 M potassium chloride solution was prepared for investigating the electrochemical characteristics of the different modified sensors. The electrolyte solution was deoxidized by flowing nitrogen gas (N_2) for 5 min before running all voltammetric measurements.

2.2. Apparatus

A CorrTest CS300 (China) electrochemical analyzer was used to perform a three-electrode system for voltammetric measurements with Ag/AgCl, GCE, and Pt-wire as reference, working, and counter electrodes, respectively. Surface characteristics of various functionalized electrodes were investigated by SEM (ZEISS Gemini 500, UK) and UV–vis (UV-1900i, Shimadzu, Japan). EIS studies were executed to investigate the impedance changes of different functionalized electrodes and recorded using DropSens μStat-i 400 s (Metrohms, Switzerland).

2.3. Synthesis of ZnO hollow sphere

The ZnO hollow sphere was fabricated by following a previously reported procedure by Ge et al. (2011) with a slight modification (Ge et al., 2011). Briefly, a 100 ml aqueous solution of a mixture of 15 mol L^{-1} Zn (NO_3)$_2$.6H$_2$O, 15 mol L^{-1} of $C_6H_{12}N_4$, and 4.08 mol L^{-1} of $C_6H_5Na_3O_7 \cdot 2H_2O$ were transferred into a flask. The flask was then sealed and placed in an oven at 90 °C for 2 h. Once the reaction was completed, the white-color precipitate was collected by centrifuging at 5000 rpm after naturally cooled down. To remove the impurities, the resulting ZnO was rinsed few times with ultrapure water and left to dry at 60 °C for 24 h. The ZnO was annealed at 400 °C for 2 h and then ground to produce the hollow ZnO.
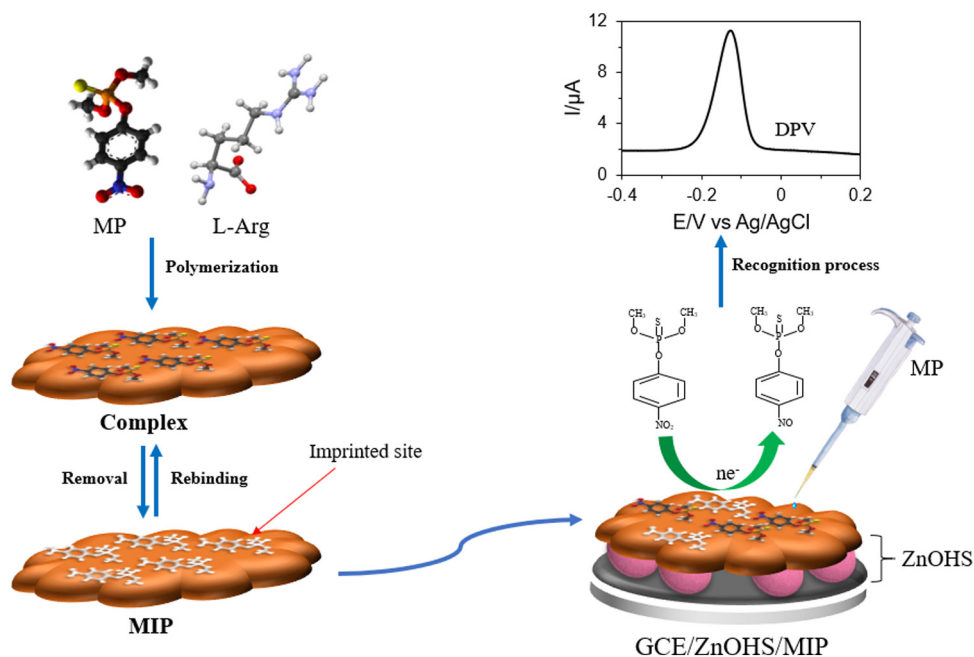
Scheme 1. The schematic procedure of GCE/ZnOHS/MIP formulation and recognition of MP.

2.4. Formulation of GCE/ZnOHS

GCE surface was first polished using a microfiber polishing pad with alumina powder (particle size of 0.3 μm) for a minute and washed with ultrapure water. Next, GCE was cleaned with ethanol and water solution, and then ultra-sonicated for 3 min. Subsequently, cyclic voltammetry (CV) was performed to treat the GCE in H_2SO_4 solution in a range of −1.0 to 1.0 V at a 0.1 V/s scant rate for 23 cycles. Following, a 10 μL suspension of ZnOHS (1 mg/ml of ZnOHS in PBS) was deposited on the GCE using the drop-casting technique. Next, the electrode (GCE/ZnOHS) was left to dry at room temperature (RM).

2.5. Formulation of GCE/ZnOHS/MIP and GCE/ZnOHS/ NIP

The CV was performed to electropolymerized both the MIP and NIP sensors. The MIP film is fabricated by polymerization of L-Arg and MP together and removal of MP using NaOH for the polymeric surface. The PBS (pH = 7.4) solution of 0.01 mol/L with 0.5×10^{-2} mol/L L-Arg and 0.5×10^{-3} mol L^{-1} MP was treated with nitrogen gas for 4 min to deoxidize the solution. To fabricate MIP film, the GCE /ZnOHS electrode was immersed in deionized PBS solution and performed CV at a scanning rate of 100 mV/s for 12 cycles in the potential range of −2.0 to 2.0 V. The electropolymerized electrode was dipped in 0.25 mol/L NaOH for 5 min to extract the template molecules and was rinsed with ultrapure water. The electrode was left to dry at RM and used as GCE/ZnOHS/MIP sensor. The preparation steps of GCE/ZnOHS/MIP are presented in Scheme 1. While the non-imprinted polymer (GCE/ZnOHS/NIP) electrode was formed similarly, but with adding no MP.

2.6. Preparation procedure of real samples

Garden-fresh strawberry, tomato, cabbage, and green beans were purchased from a local market and rinsed with ultrapure water. Each sample was cut into small pieces and homogenized by a blender to prepare the real sample. The homogenized mixture was filtered using filter paper. Finally, 200 μL of each filtered sample was diluted by adding 9.8 mL of 0.01 mol/L PBS (pH level of 7.4) solution and used as a stock solution for analysis.

3. Results and discussion

3.1. Constructional characterization of GCE/ZnOHS/MIP sensor

The CV measurements for the electro-polymerization of 5×10^{-3} mol/L L-Arg were performed in a potential range of 2 to 2 V with a scanning rate of 0.1 V/s for 12 cycles. The continuous electrodeposition of poly (L-Arg) on the GCE/ZnOHS
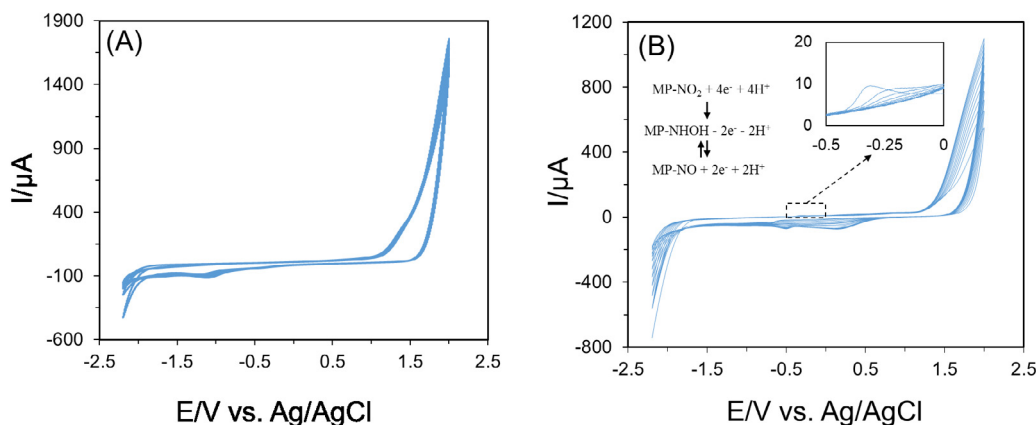
Fig. 1. (A) CV measurements for the electro-polymerization of 0.5×10^{-2} mol/L L-Arg (in 0.01 mol/L PBS at pH = 7.4) at the GCE/ZnOHS surface and (B) CV measurements for the electro-polymerization of 0.5×10^{-2} mol/L L-Arg (in 0.01 mol/L PBS at pH = 7.4) with 5.0×10^{-4} mol/L MP in a potential range of -2 to 2 V with a 100 V/s scanning rate of 12 cycles. Inset shows the electrochemical reaction mechanism.

is presented in Fig. 1A. The electrodeposition of P-Arg forms a non-conductive layer on the GCE/ZnOHS and that was validated by observing a rise in the oxidation peak currents throughout the CV measurements (Khan et al., 2018). In contrast, the electro-polymerization of 0.5×10^{-2} mol/L of L-Arg and the template molecule (MP) on the GCE/ZnOHS was carried out under the same voltammetry conditions as seen in Fig. 1B. The oxidation peaks were detected at the first cycle with a sharp anodic peak revealed at -0.20 V confirming the presence of MIP film on the GCE/ZnOHS.

3.2. Surface morphology of modified electrodes

The surface topography of GCE/ZnOHS, GCE/ZnOHS/MIP, and GCE/ZnOHS/NIP were investigated through SEM and UV–vis spectroscopy. Fig. 2 (A) shows SEM images of the as-synthesized hollow shape ZnO on the surface of GCE. The spheres possess coarse surface with diameter distribution of 0.5 to 2 μm and wall thickness of less than 100 nm. Fig. 2(B, C) represents the SEM image of the NIP and MIP modified electrode. The deposition of P-Arg (Fig. 2(B)) on the surface of the functionalized electrode is confirmed by the net-like regular and interconnected structure of P-Arg and that agrees with previously reported results (Ali et al., 2020; Khan et al., 2018). The irregular structure (Fig. 2(C)) on the surface GCE/ZnO/MIP indicates the removal of the template MP.

Fig. 2(D) shows the UV–vis spectroscopy of MP, P-Arg + MP, and ZnOHS + P-Arg + MP. MP exhibits a sharp peak at 275 nm and that is similar to the peak value that was previously reported (Mahar et al., 2020). Surprisingly, a significant decrease in absorption peak intensity is observed at 275 nm for P-Arg + MP and ZnOHS + P-Arg + MP which reveals the presence of P-Arg and ZnOHS on the surface of MP. In the case of ZnOHS + P-Arg + MP, an absorption band at 378 nm represents the presence of ZnOHS with an unshifted band of MP at 275 nm (Fageria et al., 2014).

3.3. Electrochemical characterization of GCE/ZnOHS/MIP sensor

The electrochemical-response of various functionalized electrodes was characterized by CV in a 0.5×10^{-2} mol L^{-1} [Fe(CN)$_6$]$^{3-/4-}$ solution that contains 1×10^{-1} mol/L potassium chloride as demonstrated in Fig. 3(A). The [Fe (CN)$_6$]$^{3-/4-}$ solution acted as an intermediary between different modified electrodes and substrate solutions and assisted in evaluating the voltammetric responses of electrodes (Arotiba et al., 2011). All modified electrodes showed a couple of well-defined redox peaks throughout the cyclic voltammograms. The peak potential difference (ΔE_p) of the bare GCE was 184 mV, indicating a poor electrical conductivity toward the electrode surface. However, the ΔE_p value of the ZnOHS modified GCE was decreased to 93 mV. This phenomenon indicated that ZnOHS has good electrical conductivity. In contrast, after performing the template extraction step, the ΔE_p value of GCE/ZnOHS/MIP increased to 149 mV and that suggesting a low transfer of electrons due to the decrease in polymer conductivity (Duan et al., 2019; El Jaouhari et al., 2020). The CVs of GCE/ZnOHS/MIP at various scanning rates from 0.02 to 0.15 V/s were performed in 0.5×10^{-2} mol/L [Fe(CN)$_6$]$^{3-/4-}$ containing 1×10^{-1} mol/L potassium chloride solution to study the electrochemical-behavior of the sensor. The redox peak current was observed to be proportional to the scanning rate as seen in Fig. 3B, C. Furthermore, the linear formula can be written as Ipa (y) = 0.515x + 47.491 (R^2 = 0.9858) and Ipc (y) = -0.4354x $-$ 48.958 (R^2 = 0.9886). This result indicated a surface-confined electrochemical phenomenon of the process. Moreover, EIS studies were employed in 0.5×10^{-2} mol/L [Fe(CN)$_6$]$^{3-/4-}$ solution that contains 1×10^{-1} mol/L potassium chloride to characterize impedance changes in the functionalized electrodes as seen in Fig. 3D. The Nyquist impedance spectrum consisted of two parts. The semi-circular part represents the charge-transfer-resistance (R_{ct}) and the linear part represents the diffusion process. Bare GCE had R_{ct}
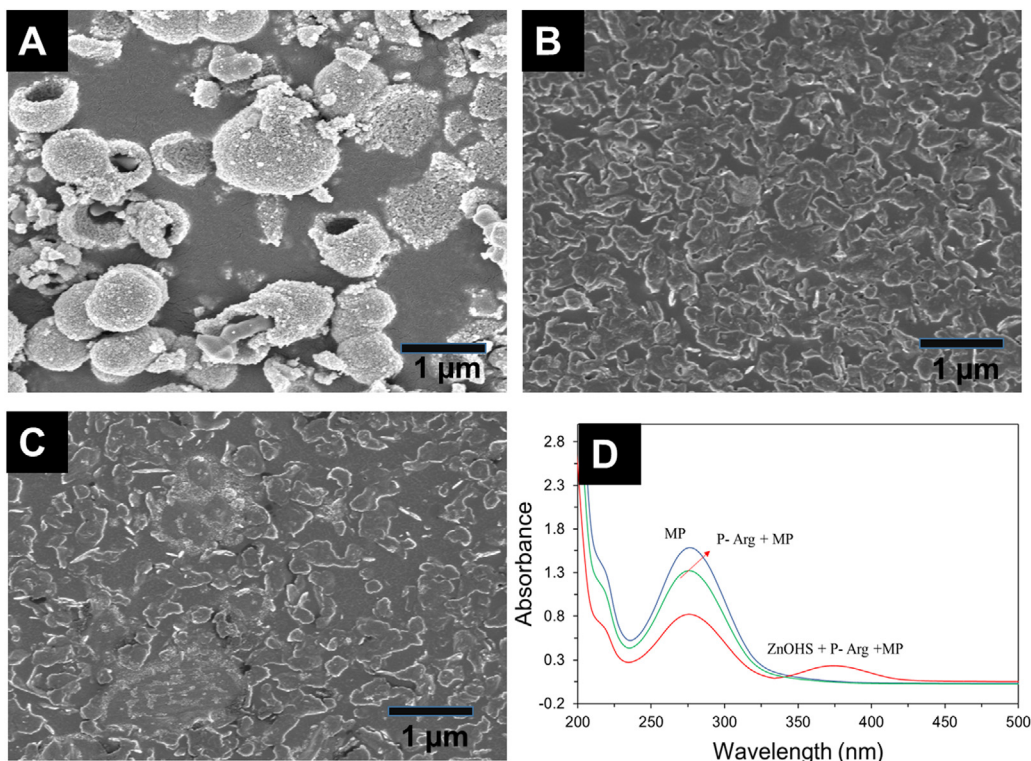
Fig. 2. SEM images of (A) ZnOHS, (B) GCE/ZnOHS/NIP electrode, (C) GCE/ZnOHS/MIP electrode and (D) UV–vis spectrum of MP, P-Arg + MP and ZnOHS + P-Arg + MP.

value of 529 Ω, while the R_{ct} value of the GCE/ZnOHS was 33 Ω. This result indicates that introducing ZnOHS successfully enhanced electron transfer rate and conductivity of the electrode. While, a higher value of R_{ct} was found for MIP (288.2 Ω) as compared to NIP (102 Ω), suggesting slow electron-transfer kinetics with recognition cavities.

3.4. Optimization of analytical conditions

3.4.1. pH effect
The pH effect of 0.01 mol/L PBS on the electrochemical signal of GCE/ZnOHS/MIP sensor toward 1.0×10^{-5} mol/L MP was investigated between pH 5.0 to 9.4 as seen in Fig. 4A. It was found that the peak current of the MP increased with the increase of the pH levels from 5 to 7.4 and it decreased for pH levels from 8.2 to 9.4. This observation indicates that the acidic electrolyte solution is more suitable for MP reduction than the basic electrolyte solution. Furthermore, the maximum current signal of MP was achieved at an optimal pH level of 7.4.

3.4.2. Template: Monomer ratio
The efficiency of the MIP sensor depends on the template and monomer (t: m) ratio used during electropolymerization (Ali et al., 2021a,b; Rezaei et al., 2013). The concentration of monomers was optimized by incorporating 0.5×10^{-3} mol/L MP with the different molar ratios of monomers such as 1:1, 1:5, 1:10, 1:15, and 1:20 (t: m). As the ratio increases from 1: 1 to 1:10, the current signal also increases and that indicates that a large number of recognition sites were generated on the electrode surface as shown in Fig. 4B. However, when the ratio further increases, the current signal decreases at a noticeable rate which may be due to an insufficient number of recognition sites being generated. The maximum current was achieved at 1: 10 that was selected for the best performance of the sensor.

3.5. Electrochemical detection of MP

Electrochemical sensing of MP was performed by DPV using optimal conditions. The electrochemical response of the functionalized electrodes for the detection of 0.1×10^{-4} mol/L MP in 0.01 mol/L PBS (pH level of 7.4) is shown in Fig. 5A. The maximum peak-current was recorded for GCE/ZnOHS/MIP sensor compared with other electrodes. For the linearity evaluation of the GCE/ZnOHS/MIP sensor, DPV was carried out for several concentrations of MP as seen in Fig. 5B. The peak-current increased with the increase of MP concentration in the range of $0.5 \times 10^{-8} - 0.1 \times 10^{-4}$ mol/L, as shown in
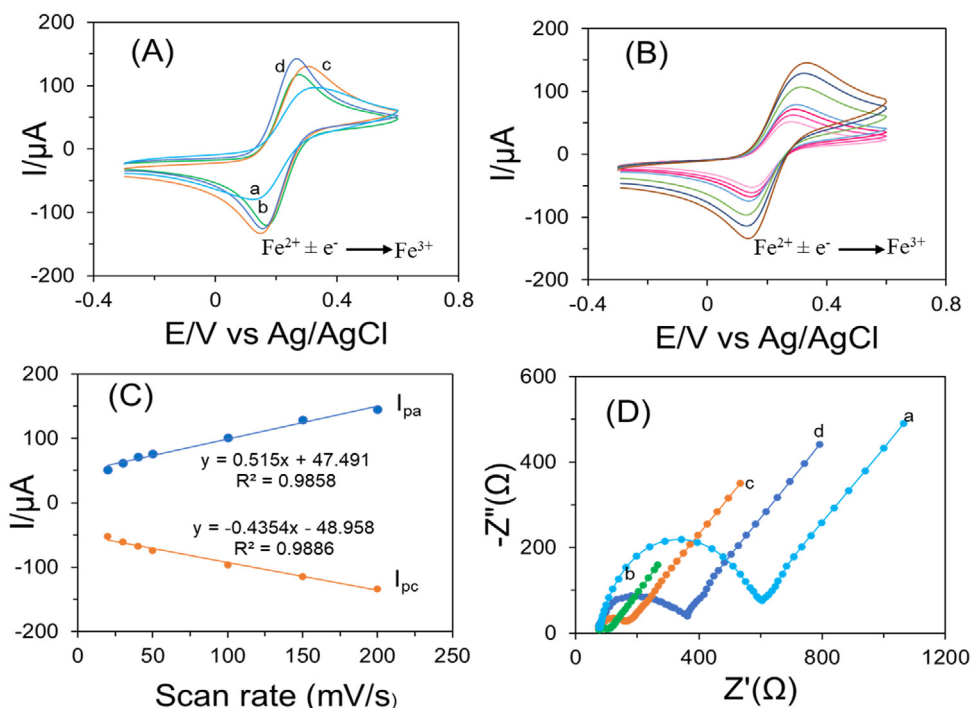
Fig. 3. (A) CV of the various electrodes: (a) unmodified GCE, (b) GCE/ZnOHS, (c) GCE/ZnOHS/NIP, and (d) GCE/ZnOHS/MIP at 100 V/s scan rate. (B) CV results for GCE/ZnOHS/MIP detector at various scanning rates (from outer to inner): 0.15, 0.1, 0.05, 0.04, 0.03 and 0.02 V/s (inset shows electrochemical reaction mechanism of oxidation and reduction) (C) resultant calibration-plots among different scanning rate vs. cathodic and anodic peak currents. (D) EIS of the various electrodes: (a) unmodified GCE, (b) GCE/ZnOHS, (c) GCE/ZnOHS/NIP, and (d) GCE/ZnOHS /MIP. All measurements were employed in 0.5×10^{-2} mol/L $[Fe(CN)_6]^{3-/4-}$ solution that contains 1×10^{-1} mol/L potassium chloride.
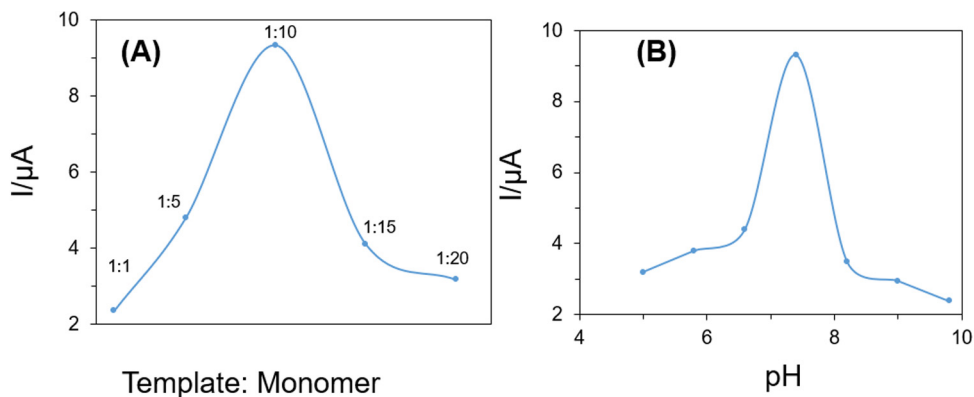

Fig. 4. (A) The pH effect of PBS on the electrochemical signal of GCE/ZnOHS/MIP sensor to 0.1×10^{-4} mol/L MP and (B) Electrochemical-behavior of the GCE/ZnOHS/MIP sensor in 5.0×10^{-4} mol/L MP with the different molar ratio of monomers such as 1:1, 1:5, 1:10, 1:15 and 1:20 (t: m).

the analytical plot of Fig. 5B. The calibration-curve is y = 0.571x + 3.698 ($R^2 = 0.985$) with a detection-limit (S/N = 3) of 0.5×10^{-9} mol/L and sensitivity of 571 nA/μ mol L^{-1} cm^{-2} which was determined by following the similar as reported previously (Ali et al., 2021a,b). Moreover, the experimental findings of the GCE/ZnOHS/MIP sensor were compared with other recently reported sensing mechanisms for the sensing of MP as shown in Table 1.

3.6. Selectivity, reproducibility and stability study

The performance of the GCE/ZnOHS/MIP detector was re-evaluated through selectivity and reproducibility analysis. Residues of the chemical are usually found unitedly in the environment, so the effects of the compounds associated with it need to be studied and that may ultimately interfere with the analysis. Thus, selectivity analysis was carried out by
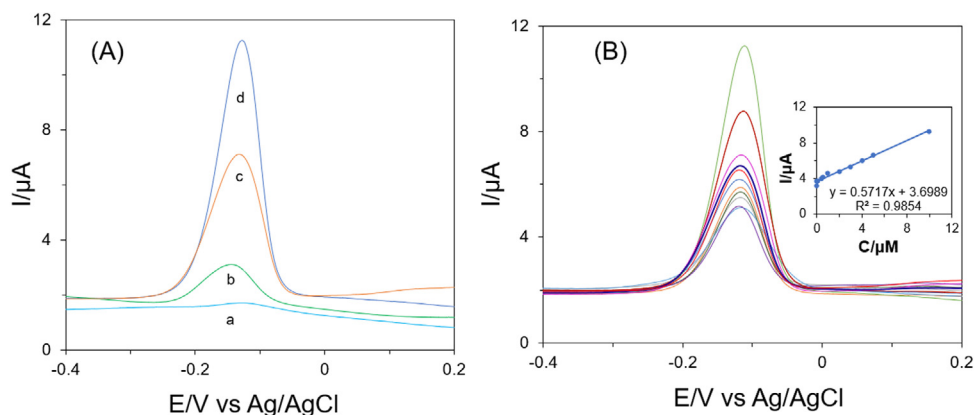
Fig. 5. (A) DPV of 1×10^{-2} mol/L MP at various electrodes: (a) unmodified GCE, (b) GCE/ZnOHS/NIP, and (c) GCE/ZnOHS/MIP in 0.01 mol/L PBS (pH level of 7.4) with a scanning rate of 100 V/s. (B) DPV responses of the GCE/ZnOHS/MIP sensor in 0.01 mol/L PBS (pH level of 7.4) at 100 V/s scan rate with linear MP concentrations range of $0.5 \times 10^{-8} - 0.1 \times 10^{-4}$ mol L^{-1}. The inset displays the calibration-curve of MP detected by the GCE/ZnOHS/MIP for all concentrations.

Table 1
Comparing the developed detector with other recently reported sensing mechanisms for sensing MP.

Electrode	Detection condition (pH)	Method	Linear range (mol/L)	Detection limit (mol/L)	Reference
MWCNTs/MIP	5.0	DPV	2.0×10^{-7} to 1.0×10^{-5}	6.7×10^{-8}	Zhang et al. (2012)
ERGO/GCE	7.0	SWV	3.0×10^{-8} to 2×10^{-9}	8.87×10^{-10}	Jeyapragasam et al. (2013)
Poly(safranine)/GCE	6.0	LSV	3.43×10^{-8} to 3.43×10^{-5}	1.0×10^{-8}	Liu (2011)
MIP-IL-EGN/GCE	6.8	DPV	1.0×10^{-8} to 7.0×10^{-6}	6.0×10^{-9}	Zhao et al. (2013)
GCE/ZnOHS/MIP	7.4	DPV	5.0×10^{-9} to 1.0×10^{-5}	5×10^{-10}	Current work

Table 2
The recovery results of PM detection in real samples utilizing the standard addition method.

Sample	Added (mol/L)	Found (mol/L)	Relative recovery (%)
Green beans	1.0×10^{-5}	9.04×10^{-6}	90.4
Strawberry	1.0×10^{-5}	9.19×10^{-6}	91.9
Tomato	1.0×10^{-5}	11.8×10^{-6}	118
Cabbage	1.0×10^{-5}	9.63×10^{-6}	96.3

introducing 200-fold of several metal ions and compounds such as Na$^+$, K$^+$, Ca^{2+}, Mg^{2+}, Cl$^-$, NO$_3^-$, SO$_4^{2-}$, p-nitrophenol, and hexaconazole with the target analyte. In the presence of all these ions, very little change ($<6\%$) was observed in the DPV response of MP. Besides, the reproducibility of the GCE/ZnOHS/MIP detector was executed using the same electrode for the repetitive determination of MP. There was no deviation ($<1\%$) found in the DPV response for several concentrations of the target analyte and that verified the suitability of the GCE/ZnO-HNS/MIP detector for the sensing of MP. Moreover, the stability of the developed detector was examined by evaluating the DPV results of 1×10^4 mol/L MP in 0.01 mol/L PBS (pH level of 7.4). This experiment was performed every 7 days over 14 days under the optimal experimental conditions. The sensor was kept in a refrigerator at 4 °C for the entire duration of the experiment. The current response of the sensor was obtained up to 98.36% after 7 days, while 94% of its actual response was obtained after 14 days. This result indicates the great stability of the GCE/ZnOHS/MIP sensing system.

3.7. Analysis of real sample

To ensure the applicability of the MIP detector, a recovery test was obtained utilizing the method of the standard addition to analyzing the real sample. The recovery results for MP determination in real samples are summarized in Table 2. The recoveries were 90.4%, 91.9%, 118%, and 96.3% for fresh green beans, strawberry, tomato, and cabbage, respectively, as Table 2. This satisfactory result suggests that the developed MIP sensor has a good potential for real sample applications.

4. Conclusions

In this work, ZnOHS arrayed MIP-based sensitive electrochemical sensor for detecting MP was successfully developed. The introduction of ZnO on GCE effectively enhanced the sensitivity of the sensor. The developed GCE/ZnOHS/MIP sensor

displayed a detection response with high sensitivity and selectivity to MP. A good linear range of 5.0×10^{-9} to 1.0×10^{-5} mol/L with a detection limit (S/N = 3) of 5.0×10^{-10} mol/L was obtained throughout the DPV experiments under the optimized conditions. The developed GCE/ZnOHS/MIP sensor was effectively detected MP in real samples with satisfying recovery results. Furthermore, the developed detector displayed good stability, sensitivity, and reproducibility to MP.

Declaration of competing interest

The authors declare that they have no known competing financial interests or personal relationships that could have appeared to influence the work reported in this paper.

Acknowledgment

References

Alenezi, M.R., Henley, S.J., Emerson, N.G., Silva, S.R.P., 2014. From 1D and 2D ZnO nanostructures to 3D hierarchical structures with enhanced gas sensing properties. Nanoscale 6, 235–247. http://dx.doi.org/10.1039/c3nr04519f.

Alexander, M., Suriyadharshini, S., Raghu, S., Kalaivani, R.A., Gnanam, S., 2019. Semiconducting material of pure ZnO hollow nanospheres; and their modified electrode used for electrocatalytic reduction of ethanol and hydrogen peroxide. Mater. Sci. Semicond. Process. 99, 62–67. http://dx.doi.org/10.1016/j.mssp.2019.04.010.

Ali, M.R., Bacchu, M.S., Al-Mamun, M.R., Rahman, M.M., Ahommed, M.S., Aly, M.A.S., Khan, M.Z.H., 2021a. Sensitive MWCNT/P-Cys@MIP sensor for selective electrochemical detection of ceftizoxime. J. Mater. Sci. 56, 12803–12813. http://dx.doi.org/10.1007/s10853-021-06115-6.

Ali, M.R., Bacchu, M.S., Daizy, M., Tarafder, C., Hossain, M.S., Rahman, M.M., Khan, M.Z.H., 2020. A highly sensitive poly-arginine based MIP as an electrochemical sensor for selective detection of dimetridazole. Anal. Chim. Acta 1121, 11–16. http://dx.doi.org/10.1016/j.aca.2020.05.004.

Ali, M.R., Bacchu, M.S., Setu, M.A.A., Akter, S., Hasan, M.N., Chowdhury, F.T., Rahman, M.M., Ahommed, M.S., Khan, M.Z.H., 2021b. Development of an advanced DNA biosensor for pathogenic Vibrio cholerae detection in real sample. Biosens. Bioelectron. 188, 113338. http://dx.doi.org/10.1016/j.bios.2021.113338.

Ameen, S., Akhtar, M.S., Seo, H.K., Shin, H.S., 2015. An electrochemical sensing platform based on hollow mesoporous ZnO nanoglobules modified glassy carbon electrode: Selective detection of piperidine chemical. Chem. Eng. J. 270, 564–571. http://dx.doi.org/10.1016/j.cej.2015.02.052.

Anh, D.H., Cheunrungsikul, K., Wichitwechkarn, J., Surareungchai, W., 2011. A colorimetric assay for determination of methyl parathion using recombinant methyl parathion hydrolase. Biotechnol. J. 6, 565–571. http://dx.doi.org/10.1002/biot.201000348.

Arotiba, O.A., Baker, P.G., Mamba, B.B., Iwuoha, E.I., 2011. The application of electrodeposited poly(propylene imine) dendrimer as an immobilisation layer in a simple electrochemical DNA biosensor. Int. J. Electrochem. Sci. 6, 673–683.

Barr, D.B., Barr, J.R., Maggio, V.L., Whitehead, R.D., Sadowski, M.A., Whyatt, R.M., Needham, L.L., 2002. A multi-analyte method for the quantification of contemporary pesticides in human serum and plasma using high-resolution mass spectrometry. J. Chromatogr. B 778, 99–111. http://dx.doi.org/10.1016/S0378-4347(01)00444-3.

Beluomini, M.A., da Silva, J.L., Sedenho, G.C., Stradiotto, N.R., 2017. D-mannitol sensor based on molecularly imprinted polymer on electrode modified with reduced graphene oxide decorated with gold nanoparticles. Talanta 165, 231–239. http://dx.doi.org/10.1016/j.talanta.2016.12.040.

De Souza, D., Machado, S.A.S., 2006. Study of the electrochemical behavior and sensitive detection of pesticides using microelectrodes allied to square-wave voltammetry. Electroanalysis 18, 862–872. http://dx.doi.org/10.1002/elan.200603480.

Duan, D., Yang, H., Ding, Y., Li, L., Ma, G., 2019. A three-dimensional conductive molecularly imprinted electrochemical sensor based on MOF derived porous carbon/carbon nanotubes composites and prussian blue nanocubes mediated amplification for chiral analysis of cysteine enantiomers. Electrochim. Acta 302, 137–144. http://dx.doi.org/10.1016/j.electacta.2019.02.028.

El Jaouhari, A., Yan, L., Zhu, J., Zhao, D., Zaved Hossain Khan, M., Liu, X., 2020. Enhanced molecular imprinted electrochemical sensor based on zeolitic imidazolate framework/reduced graphene oxide for highly recognition of rutin. Anal. Chim. Acta 1106, 103–114. http://dx.doi.org/10.1016/j.aca.2020.01.039.

EPA, 2000. Parathion Hazard Summary 4.

Fageria, P., Gangopadhyay, S., Pande, S., 2014. Synthesis of ZnO/Au and ZnO/Ag nanoparticles and their photocatalytic application using UV and visible light. RSC Adv. 4, 24962–24972. http://dx.doi.org/10.1039/c4ra03158j.

Ge, L., Jing, X., Wang, Jun, Wang, Jing, Jamil, S., Liu, Q., Liu, F., Zhang, M., 2011. Trisodium citrate assisted synthesis of ZnO hollow spheres via a facile precipitation route and their application as gas sensor. J. Mater. Chem. 21, 10750–10754. http://dx.doi.org/10.1039/c0jm04405.

Giahi, M., Badalpoor, N., Habibi, S., Taghavi, H., 2013. Synthesis of CuO/ ZnO nanoparticles and their application for photocatalytic degradation of lidocaine HCl by the trial-and-error and taguchi methods. Bull. Korean Chem. Soc. 34, 2176–2182. http://dx.doi.org/10.5012/bkcs.2013.34.7.2176.

Gui, R., Jin, H., Guo, H., Wang, Z., 2018. Recent advances and future prospects in molecularly imprinted polymers-based electrochemical biosensors. Biosens. Bioelectron. 100, 56–70. http://dx.doi.org/10.1016/j.bios.2017.08.058.

Hieu, N.M., Kim, H., Kim, C., Hong, S.K., Kim, D., 2016. A hydrogen sulfide gas sensor based on Pd-decorated ZnO nanorods. J. Nanosci. Nanotechnol. 16, 10351–10355. http://dx.doi.org/10.1166/jnn.2016.13158.

Huang, H., Bai, W., Dong, C., Guo, R., Liu, Z., 2015. An ultrasensitive electrochemical DNA biosensor based on graphene/Au nanorod/polythionine for human papillomavirus DNA detection. Biosens. Bioelectron. 68, 442–446. http://dx.doi.org/10.1016/j.bios.2015.01.039.

Jeyapragasam, T., Saraswathi, R., Chen, S.M., Lou, B.S., 2013. Detection of methyl parathion at an electrochemically reduced graphene oxide (ERGO) modified electrode. Int. J. Electrochem. Sci. 8, 12353–12366.

Kartal, F., Çimen, D., Bereli, N., Denizli, A., 2019. Molecularly imprinted polymer based quartz crystal microbalance sensor for the clinical detection of insulin. Mater. Sci. Eng. C 97, 730–737. http://dx.doi.org/10.1016/j.msec.2018.12.086.

Khan, M.Z.H., Liu, Xiaoqiang, Tang, Y., Zhu, J., Hu, W., Liu, Xiuhua, 2018. A glassy carbon electrode modified with a composite consisting of gold nanoparticle, reduced graphene oxide and poly(L-arginine) for simultaneous voltammetric determination of dopamine, serotonin and L-tryptophan. Microchim. Acta 185, 3–12. http://dx.doi.org/10.1007/s00604-018-2979-z.

Liu, X., 2011. Electrochemical sensor for determination of Parathion based on Electropolymerization Poly(Safranine) Film Electrode. Int. J. Electrochem. 2011, 1–6. http://dx.doi.org/10.4061/2011/986494.

Liu, G., Lin, Y., 2005. Electrochemical Sensor for Organophosphate Pesticides and Nerve Agents using Zirconia Nanoparticles as Selective Sorbents phosphoric group, nitroaromatic OPs strongly bind to the. Anal. Chem. 77, 5894–5901.

Mahar, A.M., Balouch, A., Talpur, F.N., Abdullah, Panah, P., Kumar, R., Kumar, A., Pato, A.H., Mal, D., Kumar, S., Umar, A.A., 2020. Fabrication of Pt-Pd@ITO grown heterogeneous nanocatalyst as efficient remediator for toxic methyl parathion in aqueous media. Environ. Sci. Pollut. Res. 27, 9970–9978. http://dx.doi.org/10.1007/s11356-019-07548-y.

Mesterházy, ákos, Oláh, J., Popp, J., 2020. Losses in the grain supply chain: Causes and solutions. Sustain http://dx.doi.org/10.3390/su12062342.

Mulchandani, P., Chen, W., Mulchandani, A., Wang, J., Chen, L., 2001. Amperometric microbial biosensor for direct determination of organophosphate pesticides using recombinant microorganism with surface expressed organophosphorus hydrolase. Biosens. Bioelectron. 16, 433–437. http://dx.doi.org/10.1016/S0956-5663(01)00157-9.

Rezaei, B., Rahmanian, O., Ensafi, A.A., 2013. Sensing lorazepam with a glassy carbon electrode coated with an electropolymerized-imprinted polymer modified with multiwalled carbon nanotubes and gold nanoparticles. Microchim. Acta 180, 33–39. http://dx.doi.org/10.1007/s00604-012-0897-z.

Sadik, O.A., Land, W.H., Wang, J., 2003. Targeting chemical and biological warfare agents at the molecular level. Electroanalysis 15, 1149–1159. http://dx.doi.org/10.1002/elan.200390140.

Sakata, M., 2005. II.7.2 Organophosphorus pesticides. pp. 534–544.

Shanker, A., Sood, C., Kumar, V., Ravindranath, S.D., 2001. A modified extraction and clean-up procedure for the detection and determination of parathion-methyl and chlorpyrifos residues in tea. Pest Manag. Sci. 57, 458–462. http://dx.doi.org/10.1002/ps.312.

Silva, D., Cortez, C.M., Cunha-Bastos, J., Louro, S.R.W., 2004. Methyl parathion interaction with human and bovine serum albumin. Toxicol. Lett. 147, 53–61. http://dx.doi.org/10.1016/j.toxlet.2003.10.014.

Tan, X., Hu, Q., Wu, J., Li, Xiaoyu, Li, P., Yu, H., Li, Xiaoyan, Lei, F., 2015. Electrochemical sensor based on molecularly imprinted polymer reduced graphene oxide and gold nanoparticles modified electrode for detection of carbofuran. Sensors Actuators B 220, 216–221. http://dx.doi.org/10.1016/j.snb.2015.05.048.

Tomkins, B.A., Ilgner, R.H., 2002. Determination of atrazine and four organophosphorus pesticides in ground water using solid phase microextraction (SPME) followed by gas chromatography with selected-ion monitoring. J. Chromatogr. A 972, 183–194. http://dx.doi.org/10.1016/S0021-9673(02)01121-4.

Uzun, L., Turner, A.P.F., 2016. Molecularly-imprinted polymer sensors: Realising their potential. Biosens. Bioelectron. 76, 131–144. http://dx.doi.org/10.1016/j.bios.2015.07.013.

Wang, Z., Cao, X., 2015. Preparation of core–shell molecular imprinting polymer for lincomycin A and its application in chromatographic column. Process Biochem. 50, 1136–1145. http://dx.doi.org/10.1016/j.procbio.2015.04.013.

Wang, J., Chatrathi, M.P., Mulchandani, A., Chen, W., 2001. Capillary electrophoresis microchips for separation and detection of organophosphate nerve agents. Anal. Chem. 73, 1804–1808. http://dx.doi.org/10.1021/ac001424e.

Wang, D., Du, S., Zhou, X., Wang, B., Ma, J., Sun, P., Sun, Y., Lu, G., 2013. Template-free synthesis and gas sensing properties of hierarchical hollow ZnO microspheres. CrystEngComm 15, 7438–7442. http://dx.doi.org/10.1039/c3ce40812d.

Wang, Y., Yao, L., Liu, X., Cheng, J., Liu, W., Liu, T., Sun, M., Zhao, L., Ding, F., Lu, Z., Zou, P., Wang, X., Zhao, Q., Rao, H., 2019. CuCo2O4/N-Doped CNTs loaded with molecularly imprinted polymer for electrochemical sensor: Preparation, characterization and detection of metronidazole. Biosens. Bioelectron. 142, 111483. http://dx.doi.org/10.1016/j.bios.2019.111483.

Wang, J., Zhao, J., Yang, J., Cheng, J., Tan, Y., Feng, H., Li, Y., 2020. An electrochemical sensor based on MOF-derived NiO@ZnO hollow microspheres for isoniazid determination. Microchim. Acta 187, 2–9. http://dx.doi.org/10.1007/s00604-020-04305-8.

Xue, X., Wei, Q., Wu, D., Li, H., Zhang, Y., Feng, R., Du, B., De Souza, D., Machado, S.A.S., Silva, D., Cortez, C.M., Cunha-Bastos, J., Louro, S.R.W., 2004. Determination of methyl parathion by a molecularly imprinted sensor based on nitrogen doped graphene sheets. Toxicol. Lett. 18, 366–371. http://dx.doi.org/10.1002/elan.200603480.

Yang, G., White, I.M., Fan, X., 2008. An opto-fluidic ring resonator biosensor for the detection of organophosphorus pesticides. Sensors Actuators B 133, 105–112. http://dx.doi.org/10.1016/j.snb.2008.02.004.

Zhang, Z., Cai, R., Long, F., Wang, J., 2015a. Development and application of tetrabromobisphenol A imprinted electrochemical sensor based on graphene/carbon nanotubes three-dimensional nanocomposites modified carbon electrode. Talanta 134, 435–442. http://dx.doi.org/10.1016/j.talanta.2014.11.040.

Zhang, D., Yu, D., Zhao, W., Yang, Q., Kajiura, H., Li, Y., Zhou, T., Shi, G., 2012. A molecularly imprinted polymer based on functionalized multiwalled carbon nanotubes for the electrochemical detection of parathion-methyl. Analyst 137, 2629–2636. http://dx.doi.org/10.1039/c2an35338e.

Zhang, J., Zhao, B., Pan, Z., Gu, M., Punnoose, A., 2015b. Synthesis of ZnO nanoparticles with Controlled Shapes, Sizes, Aggregations, and Surface complex Compounds for tuning or Switching the Photoluminescence. Cryst. Growth Des. 15, 3144–3149. http://dx.doi.org/10.1021/cg5017017.

Zhao, L., Zhao, F., Zeng, B., 2013. Electrochemical determination of methyl parathion using a molecularly imprinted polymer-ionic liquid-graphene composite film coated electrode. Sensors Actuators B 176, 818–824. http://dx.doi.org/10.1016/j.snb.2012.10.003.